Int J Earth Sci (Geol Rundsch) (2010) 99:1731–1740
DOI 10.1007/s00531-009-0476-7

ORIGINAL PAPER

Timing of Holocene sand accumulation along the coast of central and SE Vietnam

Dam Quang-Minh · Manfred Frechen · Tran Nghi · Jan Harff

Received: 15 January 2008 / Accepted: 19 July 2009 / Published online: 21 August 2009

Abstract In Vietnam, the coastal sand barriers and dunes located in front of the steep slopes of the high rising Truong Son Mountains are sensitive to climate and environment change and give evidence for Holocene sea-level rise. The outer barrier sands were deposited shortly before or contemporaneous with the local sea-level high stand along the Van Phong Bay postdating the last glacial maximum (LGM). Optically stimulated luminescence (OSL) dating yielded deposition ages ranging from 8.3 ± 0.6 to 6.2 ± 0.3 ka for the stratigraphically oldest exposed barrier sands. Further periods of sand accumulation took place between 2.7 and 2.5 ka and between 0.7 and 0.5 ka. The youngest period of sand mobilisation was dated to 0.2 ± 0.01 ka and is most likely related to reworked sand from mining activities. At the Suoi Tien section in southern central Vietnam, the deposition of the inner barrier sands very likely correlate with an earlier sea-level high stand prior to the last glaciation. OSL age estimates range from 276 ± 17 to 139 ± 15 ka. OSL dating significantly improves our knowledge about the sedimentary dynamics along the coast of Vietnam during the Holocene.

D. Quang-Minh · T. Nghi
Faculty of Geology, University of Science,
334 Nguyen Trai, Hanoi, Vietnam
e-mail: minhdq@vnu.edu.vn

M. Frechen (✉)
Leibniz Institute for Applied Geophysics,
Section S3: Geochronology and Isotope Hydrology,
Stilleweg 2, 30655 Hannover, Germany
e-mail: Manfred.Frechen@liag-hannover.de;
Manfred.Frechen@gga-hannover.de

D. Quang-Minh · J. Harff
Baltic Sea Research Institute,
Seestr. 15, 18119 Rostock-Warnemünde, Germany

Keywords Sea-level change · Dune · Chronology · Holocene · Vietnam · Coast

Introduction

Climate change has a tremendous impact on coastal landform evolution; hence, coasts are in a process of constant change. The Holocene interglacial warming trend led to eustatic sea-level rise of about 120 m since the last deglaciation affecting the production, availability, and mobility of coastal sediments and playing a major role in the formation and shaping of recent shorelines. This sea-level high stand has persisted for the past 7,000 years (Siddall et al. 2007; Lambeck and Chappell 2001; Vink et al. 2008). Postglacial isostatic adjustments of the shorelines range in elevation from several metres above to several metres below the present sea-level (Rabineau et al. 2006; Waelbroeck et al. 2002; Vink et al. 2008). Coastal deposits are extremely sensitive to environment and climate changes, thus representing excellent archives of past climate conditions, including proxy records of annual precipitation, vegetation cover, wind strength, sediment supply, and its interrelation to sea-level changes (Frechen et al. 2004; Porat et al. 2003, 2004).

Sand-barrier shorelines, wave-cut notches, beach rocks or coral remains are examples for depositional features that occur at or close to the coast. Extensive sand barriers and dune sands are widely distributed along the southeastern and central coast of Vietnam located in the narrow coastal plain in front of the high rising Truong Son Mountains. Numerous small rivers transport large amounts of sediments from the Truong Son Mountains into the South China Sea (Fig. 1). The shelf off Central Vietnam is only 20 km wide. Thus, shoreline migration extended a few tens of kilometres inland

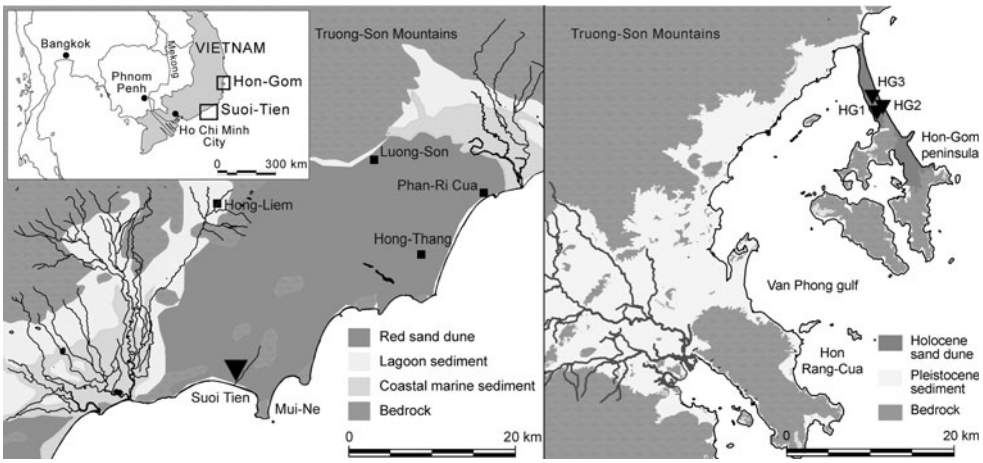

Fig. 1 Map showing the location of the two working areas in Vietnam (a). The working area at Suoi Tien (10°57′16″N and 108°15′30″E) and at Hon Gom (12°41.64′N and 109°45.27′E) are located in the southeastern and central part of Vietnam (after Tran 1996, 1998)

following sea-level rise after the last glacial maximum (LGM) (Schimanski and Stattegger 2005; Tanabe et al. 2003). During the Pleistocene, this area most likely experienced major periods of marine transgression and regression resulting in a repeated reorganisation of the depositional system. Today most of the coastal sand barriers and dune sands of the study area are stabilised by vegetation. Little is known about the timing of sand accumulation along the coast because numerical data is absent.

Holocene interglacial sea-level changes and coastal alteration have been the subject of considerable studies. Accurate and precise numerical dating is mandatory to understand local and regional issues of coastal landform evolution and sea-level change as well as ancient shore lines predating the Holocene interglacial. Radiocarbon is a widely used dating technique to date coastal organic material of the Holocene interglacial (Vink et al. 2008). Luminescence dating technique has improved considerably in the last decade, and is today a useful and robust dating technique in areas, where suitable material for other dating techniques like radiocarbon or uranium-series dating is lacking (Jacobs 2008). The improved accuracy and precision of optically stimulated luminescence (OSL) ages for Holocene deposits enable us to quantify coastal sedimentary dynamics such as the evolution of barriers and dunes and its timing.

The aim of this study is to test the suitability of Late Pleistocene and Holocene sandy coastal barriers and dune sands for OSL dating at Suoi Tien section and at Hon Gom section in the southeastern and central part of Vietnam (Fig. 1) and to set up a more reliable chronological frame for the coastal aeolian sand accumulation and its relation to sea level rise postdating the LGM.

Geological setting

The central and southeastern part of Vietnam is morphologically characterised by an elevated hinterland, which is located close to the coast, with elevations of 1,000 m above sea level (asl) to a maximum of about 2,600 m asl. Small rivers deliver large amounts of terrigenous sediments from the Truong Son Mountain Chain onto the narrow shelf. High sedimentation rates of 50–100 cm/ka and even 600–1,200 cm/ka were determined for short periods during the early Holocene (Schimanski and Stattegger 2005; Szczucinski and Stattegger 2001), as determined by numerical dating of sediments from the northern Central Shelf, which gave calibrated acceleration mass spectrometry (AMS) ^{14}C ages between 9.39 and 6.41 ka ($n = 9$) for this Holocene period. The accumulation of sediments was most likely triggered by enhanced erosion in the Truong Son Mountains owing to intensified SW monsoon, and by increasing the accommodation space on the shelf due to sea-level rise (Schimanski and Stattegger 2005). The chronology of Late Pleistocene sediments was provided by AMS ^{14}C data yielding numerical ages older than 13 ka (Schimanski and Stattegger 2005; Tanabe et al. 2003). An outer and an inner sand barrier can be distinguished along the southeastern and central coast of Vietnam. The outer sand barrier consists of loose white sand, forming morphologically bay head barriers and tombolos. The inner sand barrier consists of light yellow to reddish yellow sand.

The study area has a tropical climate characterised by seasonal change between dry and rainy periods. The humid season begins in June and ends in October, whereas the dry season lasts from November to May. The mean temperature is 27°C, the annual precipitation is 800 mm and evaporation is 1,280 mm (Le-Duc 2003). The present climate indicates a short rainy season with long dry periods resulting in sand mobility.

The Suoi Tien section consists of a succession of sand barriers and is located near the village of Suoi Tien, which is situated in the Binh Thuan province in the southern part of the central coast of Vietnam. Cretaceous rhyolite and granite are exposed about 5 km in the northeast of Suoi Tien (Fig. 1). An older sand succession is separated from

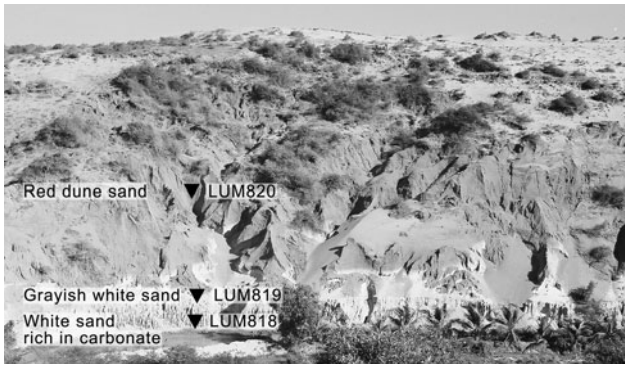

Fig. 2 Picture showing Suoi Tien section and the position of the samples LUM818–820

the younger dune sands by an extensive back-barrier mud basin (Murray-Wallace et al. 2002). The coastal sand barrier and dunes consist of thick sand accumulations and form a narrow strip of about 20 km inland. The relief of the study area is hilly and the average altitude of these dunes range from 100 to 160 m asl. The section under study is exposed in an up to 80-m deep dissected modern channel about 0.5 km inland from the present shoreline at Suoi Tien village (Fig. 2). The morphology of the study area is characterised by an up to 160-m high hilly area. The channel has cut into a succession of white, grey, and red sand, as deposited from the bottom to the top, respectively (Fig. 2). The bedrock is made up of gravel, including basalt fragments, and bottomed out in a drill hole at a depth of 27 m below the bottom of the stream (Nghi 1998).

Three units can be distinguished lithologically in the field. The lowermost one consists of homogenous, weakly layered white fine to medium quartz-rich sand and is strongly indurated by carbonate. Murray-Wallace et al. (2002) reported detrital feldspar, excluding orthoclase up to 5.5% that is partly transformed to clay. Loose, massive white quartz-rich sand up to 6 m thick discontinuously covers the grey sand. The white sand passes gradually to medium red quartz-rich (92–98%) sand. This well-sorted red sand is sometimes weakly indurated by hematite. The grains are well-rounded and partly coated with hematite suggesting chemical weathering. Bedding and cross-bedding indicate a likely accumulation of the sediment within a shallow marine environment. Nghi (1998) correlated these sediments with Middle and Late Pleistocene times, which were later confirmed by preliminary thermoluminescence age estimates for sediments from the Suoi Tien section (Murray-Wallace et al. 2002).

Three samples were taken from the sandy deposits in the lower part of the Suoi Tien section: sample LUM 818 from the basal grey sand about 72 m below the present surface; sample LUM 819 and LUM 829 were collected from the white sand about 67 m below the present surface and from the red sand about 45 m below the present surface, respectively (Fig. 2).

The Hon Gom peninsula is located in the Van Phong bay in the southeastern central part of the coast of Vietnam (Fig. 1). The tropical climate results in an annual precipitation rate of 1,800–2,000 mm spread over around 170 days per year. The tides have a strong diurnal component up to 2 m (Le-Duc 2003). The Van-Phong bay is surrounded by an up to 20 km long and about 1–2-km-wide tombolo in NW–SE direction connecting islands with the continent, and a sandy barrier on the continent extending about 60 km in SW–NE direction. The bedrock consists of Cretaceous granite, rhyolite and andesite (Nguyen 1998; Tran 1998). The source material of the dunes is transported by numerous small rivers from the Truong Son Mountains to the flat shelf area, where the sediment has been reworked and re-deposited by tidal and wave action. Dao and Nguyen (2001) correlated the formation of the sand barrier and dune sands to the sea-level rise during the Holocene. North to the study area, diatoms and foraminifera were found inland indicating marine conditions for these Pleistocene deposits.

The sand barrier from Hon Gom peninsula creates a link between the island and the continent (Fig. 3). Large sand dunes of 10–40-m thick partly cover granitic bedrock at the northern and southern end of the barrier. The sections at Hon Gom are located near the village of Dam Mon. The sediment sequences are characterised by successions of white, yellow, and reddish yellow sand (Figs. 3, 4). The dune sand is quartz-rich. Occasionally the sandy sediment is enriched by heavy minerals such as ilmenite, zircon,

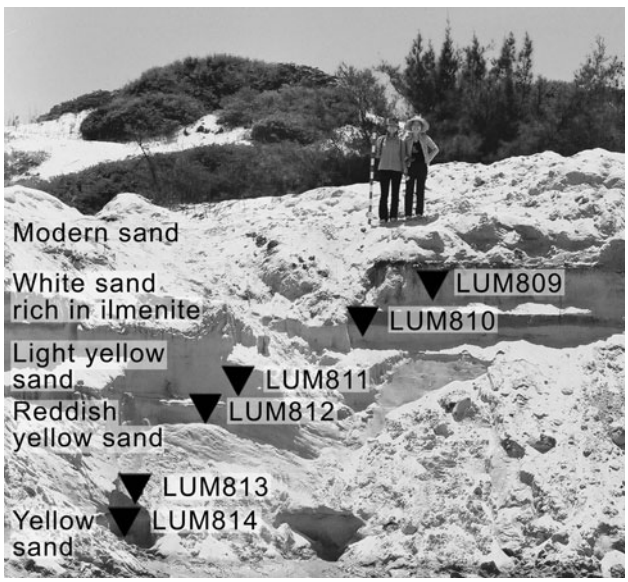

Fig. 3 Picture showing the Hon Gom 1 section and the position of the samples LUM 809–814

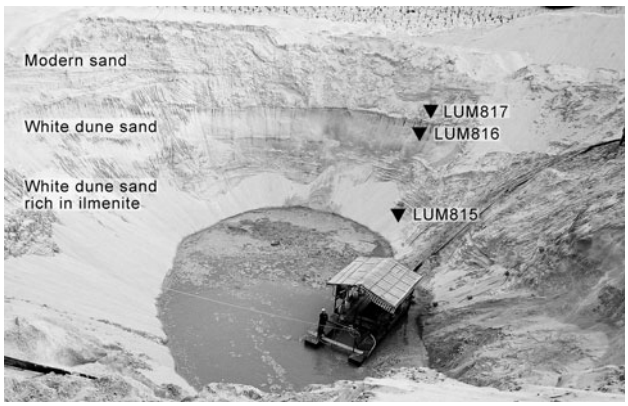

Fig. 4 Picture showing the Hon Gom 2 section and the position of the samples LUM 815–817

anatase, rutile, pyroxene, and monazite, as described by Nghi (1998) and Tran (1998). The white quartz-rich sand was excavated for glass production.

The Hon-Gom 1 section is located in the southeastern part of the tombolo (Fig. 1). The water table is at a depth of 6.50 m below surface. At the bottom of the 7-m thick sequence, bright yellow, fine to coarse quartz-rich sand with an enrichment of coarse-grained sand (1–2-mm grain size) at the bottom were deposited. The yellow sand is covered by reddish yellow fine to medium-grained quartz-rich sand with a thickness of about 1.80 m, followed by 1.50-m thick light yellow sand rich in ilmenite. The next layer to the top has a thickness of about 0.80 m and is composed of fine white sand covered by reworked sand of the mining activities. Ten samples were taken from middle to coarse grained sand. The position of the samples is provided in Fig. 3 and Table 1.

The Hon Gom 2 section is situated in the northwest of the Hon Gom 1 section. The sand deposits have a thickness of more than 10.50 m (position of the groundwater/sea-water table). In the lower part of the sequence, white horizontally layered dune sand about 7.60-m thick and rich in ilmenite is exposed. In the upper part of the unit, the sand is more homogeneous showing an erosional surface. This sand is covered by white dune sand about 1.80-m thick, which is laminated and partly cross-bedded in cm-scale. The top of the sequence is formed by a layer of homogenous white sand. Three samples were taken from the Hon-Gom 2 section. Samples LUM 815 and LUM 816 were collected from the white sand, which is rich in ilmenite, at depths of 9.00 m and 2.30 m below surface, respectively. Sample LUM 817 was taken from the white dune sand about 1.50 m below surface (Fig. 4).

The Hon Gom 3 section is located to the northwest of the Hon Gom 1 and 2 sections. Modern sand was sampled to test the bleaching characteristics of the sediment under study.

Table 1 Multiple aliquot additive dose (MAAD) protocol for feldspar grains

1. IR short shine of 0.4 s for normalisation
2. Irradiation of natural + dose aliquots
3. Delay of >40 days between irradiation and further treatment
4. Preheat of all aliquots at 230°C for 1 min
5. Measurement of IR decay curves

Luminescence dating

Luminescence dating methods have proved to be successful to determine the time elapsed since the last exposure to sunlight enabling to determine the deposition age or burial time of coastal aeolian sediments (Frechen et al. 2004; Porat et al. 2004; Kunz et al. 2009). The dating range is from a few years (e.g. Madsen et al. 2005; Kunz et al. 2009) to more than hundred thousand years (Frechen et al. 2004). Sufficient exposure to sunlight may not be a problem in most cases (Jacobs 2008). Overestimation of OSL ages owing to insufficient bleaching is unlikely for aeolian deposits such as those from the sand barriers and dunes of this study. However, beta microdosimetry variations and postdepositional mixing cannot be excluded; both would result in a greater scatter of equivalent dose values. Comprehensive reviews of luminescence dating methods are provided by Aitken (1998), Bøtter-Jensen et al. (2003), Wintle (1997), and Lian and Roberts (2006).

The samples were taken in light-tight cylinders in the field. The outer light-exposed part of the sample was removed under subdued red light in the laboratory and used for dosimetric analysis. About 150 g each sample was prepared for the luminescence measurements. The sandy sediment was sieved to separate the grain-size fractions 100–200, 150–212, and 212–250 µm. The minerals of the selected grain-size fraction, depending on the particle size distribution, were treated by 10% hydrochloric acid, 0.01 N sodium oxalate and 30% hydrogen peroxide to remove carbonate, clay coatings, and organic matter, respectively. Most of the coating of clay and ferric oxides was removed during this part of the preparation process, including treatment in ultra sonic bath.

Potassium-rich feldspars and quartz minerals were extracted from all samples by heavy liquid separation using sodium polytungstate at densities of 2.63 and 2.58 g/cm^3. The quartz fraction was treated with 40% hydrofluoric acid for 60 min to remove the outer about 10-µm thick rim of the quartz grains. After further sieving the quartz grains and the potassium-rich feldspar grains were separately fixed on aluminium discs with silicon spray.

Luminescence measurements were carried out on an automated Risø reader (OSL/TL-DA-15B/C) with an internal $^{90}Sr/^{90}Y$ beta source (0.18 Gy/s). The feldspar grains were stimulated by infrared diodes emitting at about 880 ± 80 nm. A filter combination of Schott BG-39 and Corning 7-59 was used for the feldspar separates giving a transmission window between 320 and 480 nm. Blue light diodes were used for the stimulation of the quartz at a fixed temperature of 125°C. A Hoya U-340 filter was placed between quartz separates and photomultiplier giving a transmission window centred at 340 nm.

The multiple aliquot additive dose (MAAD) protocol was applied for potassium-rich feldspars (cf. Frechen et al., 2004). A set of 48 discs were measured for each sample including naturals and 7-dose steps up to 945 Gray (Gy) including artificial bleaching of three aliquots by an unfiltered Dr. Hönle solar simulator for 3 h. The equivalent dose (D_e) was obtained by calculating the 1–5 s integral of the IRSL decay curves using the three bleached aliquots for background subtraction.

Furthermore, the D_e values were determined by applying the single aliquot regenerative (SAR) protocol (Murray and Wintle 2000; Wallinga et al. 2000) for both monomineralic potassium-rich feldspar and quartz-rich separates (Table 2). Due to the variability of quartz and feldspar luminescence properties and the variety of geological processes during sediment transport and deposition, the suitable measurement conditions have to be validated for at least one sample in each exposure assuming that the sediment source remains the same for the sequence. Sets of 24 discs were measured for each sample. A dose–response curve with typically three dose points is measured on a single aliquot by repeated irradiations, preheats, and OSL stimulations (IR and blue light). Sensitivity changes occurring due to laboratory heat treatment are monitored after OSL stimulation and corrected. To avoid thermal transfer effects, preheat plateau tests were carried out for two samples, including a temperature range from 200 to 300°C (Fig. 5). A preheat temperature of 240°C was applied for natural and regenerative doses. The OSL test dose response was measured at a preheat temperature of 210°C followed by immediate cooling. The cut heat was set for 10 s at 210°C for feldspars, and 210°C with immediate cooling for quartz. The IRSL response was measured for 300 s at 50°C and the OSL was measured for 40 s at 125°C. The weighted mean D_e value and the error of the weighted mean were calculated from 24 aliquots for most of the samples, for both feldspar and quartz grains. Aliquots were taken into account, when the natural signal was between first and second artificial dose step and the recycling ratio was between 0.8 and 1.2. The recycling ratio is a test for the effectiveness of the sensitivity correction and determined by repeating the first dose point in the growth curve at the end of the measured cycle. Murray and Wintle (2000) suggested that aliquots should be rejected, if the recycling ratios are outside 10% of unity.

Tests for feldspar contamination were carried out by IR stimulation prior to stimulation by blue light. The blue stimulation of the quartz separates of samples LUM 810 and LUM 814 gave between 1,000 and 12,000 counts, whereas IR stimulation yielded only between 20 and 80 counts indicating a negligible contamination by feldspar. D_e values were determined using the software analyst (G.A.T. Duller, Aberystwyth).

The dose-rate was calculated from potassium, uranium, and thorium contents, as measured by high-resolution gamma spectrometry using bulk samples and assuming radioactive equilibrium for the decay chains (Table 3). A more detailed description of the dosimetry as measured by gamma spectrometry is provided by Kunz et al. (2009).

Table 2 Single aliquot regenerative (SAR) protocol, as applied for both quartz (OSL stimulation) and feldspar grains (IRSL stimulation) (after Murray and Wintle 2000; Wallinga et al. 2000)

1. Preheat of natural
2. IRSL decay of naturals for 300 s at 50°C/OSL decay for 40 s at 125°C
3. Test dose (10 s)
4. Preheat test dose [cut heat at 210°C for 10 s (feldspar), and 210°C for 0 s (quartz)]
5. Measurement of test dose (IRSL decay for 300 s at 50°C for feldspar/OSL decay for 40 s at 125°C for quartz)
6. Regenerative dose of 40 s
7. Preheat of regenerative dose for 10 s at 210°C
8. IRSL decay of regenerative dose for 300 s at 50°C/OSL decay for 40 s at 125°C
9. Test dose for 10 s
10. Preheat test dose [cut heat at 210°C for 10 s (feldspar), and 210°C for 0 s (quartz)]
11. IRSL decay for 300 s at 50°C/OSL decay for 40 s at 125°C
12. Repeat step 6–11 for R2, R3, zero point and recycling point, etc.

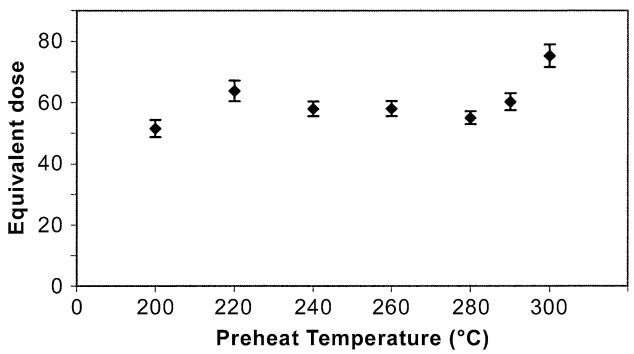

Fig. 5 D_e values, as determined by the SAR protocol applying 10 s preheat at 20°C intervals ranging from 200 to 300°C for sample LUM 814

Table 3 Dosimetric results, as determined for samples from Hon Gom 1-3 sections and Suoi Tien section

Sample	Lab-Id. LUM	Depth (m)	Grain-size (μm)	Uranium (ppm)	Thorium (ppm)	Potassium (%)	Cosmic dose (μGy/a)	H_20 (%)	Dose rate Feldspar (Gy/ka)	Dose rate Quartz (Gy/ka)
HG1-1	809	2.0	225 ± 25	1.11 ± 0.04	5.03 ± 0.08	0.54 ± 0.02	151 ± 8	7 ± 3	2.12 ± 0.11	1.19 ± 0.05
HG1-2	810	2.5	200 ± 50	0.64 ± 0.04	2.05 ± 0.06	0.57 ± 0.02	148 ± 7	7 ± 3	1.69 ± 0.16	0.93 ± 0.04
HG1-3	811	3.9	181 ± 31	0.74 ± 0.03	2.82 ± 0.07	0.62 ± 0.02	141 ± 7	15 ± 5	1.67 ± 0.12	0.96 ± 0.06
HG1-4	812	4.0	225 ± 25	0.64 ± 0.04	2.33 ± 0.06	0.70 ± 0.02	141 ± 7	15 ± 5	1.80 ± 0.11	0.96 ± 0.06
HG1-5	813	5.2	200 ± 50	0.95 ± 0.03	3.12 ± 0.06	0.91 ± 0.02	135 ± 7	20 ± 5	1.95 ± 0.17	1.16 ± 0.08
HG1-6	814	6.0	225 ± 25	0.86 ± 0.03	3.22 ± 0.07	1.07 ± 0.02	132 ± 7	25 ± 5	1.96 ± 0.17	1.19 ± 0.08
HG2-1	815	10.2	181 ± 31	1.00 ± 0.05	4.98 ± 0.09	0.53 ± 0.02	114 ± 6	25 ± 5	1.66 ± 0.13	0.91 ± 0.06
HG2-2	816	2.1	175 ± 25	2.44 ± 0.02	13.11 ± 0.7	0.50 ± 0.01	151 ± 8	7 ± 3	3.06 ± 0.23	1.99 ± 0.08
HG2-3	817	1.8	200 ± 50	1.09 ± 0.05	4.47 ± 0.09	0.39 ± 0.02	152 ± 8	7 ± 3	1.87 ± 0.16	1.03 ± 0.04
ST1	818	72.0	225 ± 25	1.45 ± 0.03	5.24 ± 0.05	0.93 ± 0.01	25 ± 1	15 ± 7	2.28 ± 0.18	1.35 ± 0.13
ST2	819	67.0	200 ± 50	0.64 ± 0.02	2.29 ± 0.04	0.18 ± 0.01	28 ± 1	4 ± 2	1.27 ± 0.17	0.49 ± 0.02
ST3	820	45.0	150 ± 50	1.02 ± 0.02	4.11 ± 0.05	0.05 ± 0.01	44 ± 1	4 ± 2	1.28 ± 0.15	0.62 ± 0.02
HG3-1	821	2.0	181 ± 31	3.64 ± 0.03	20.81 ± 0.09	0.37 ± 0.01	151 ± 8	7 ± 3	3.96 ± 0.33	2.66 ± 0.10

An average internal potassium content of 12 ± 0.5% was applied for all feldspar (Huntley and Barril 1997). Cosmic dose was corrected for the altitude and sediment thickness, as described by Prescott and Hutton (1994). The natural moisture of the sediment was estimated between 10 ± 2 and 25 ± 5% for all samples depending on the depth below surface and the position of the present water table. Dosimetric results, D_e values and IRSL/OSL age estimates are presented in Tables 3 and 4.

Results

Uranium, thorium, and potassium contents range from 0.6 to 3.6 ppm, from 2.1 to 20.8 ppm, and from 0.2 to 1.1%, respectively, for the samples from the Hon Gom peninsula (Table 3). The dose rate is between 1.3 and 4.0 Gy/ka resulting in a mean dose rate of 2.04 Gy/ka for feldspar separates and between 0.5 and 2.7 Gy/ka with a mean dose rate of 1.19 Gy/ka for quartz separates. Sample HG3-1 shows significantly higher uranium and thorium content than the remaining samples most likely owing to enrichment of heavy minerals like monazite.

The D_e values of the potassium-rich feldspar separates range from 6.6 ± 2.4 to 8.5 ± 2.5 Gy (MAAD) and from 3.9 ± 0.1 to 9.8 ± 0.2 Gy (SAR) resulting in IRSL age estimates between 1.5 ± 0.3 and 4.5 ± 1.0 ka (MAAD) and between 0.2 ± 0.1 and 5.0 ± 0.5 ka (SAR) (Table 4). Owing to the large standard deviation no age increase with depth was determined by the MAAD protocol, whereas the IRSL age estimates, as determined by the SAR protocol, show an excellent age increase with depth owing to higher precision and accuracy. The quartz separates yielded D_e values ranging from 6.1 ± 0.1 to 9.6 ± 0.3 Gy resulting in OSL age estimates between 6.2 ± 0.5 and 8.3 ± 0.6 ka. The OSL age estimates indicate no age increase with depth except for the youngest samples.

At the Hon Gom 2 section, three samples were investigated. The D_e values show a large scatter for the two youngest sediments, most likely owing to the high background/signal ratio. The latter two results are excluded from further interpretation. The lowermost sample HG2-1 yielded a D_e value of 7.3 ± 1.6 Gy resulting in an IRSL age estimate of 4.4 ± 1.0 ka. The D_e values, as determined by the SAR protocol, range from 0.3 ± 0.1 to 7.8 ± 0.1 Gy resulting in IRSL age estimates between 0.2 ± 0.1 and 4.7 ± 0.4 ka showing an excellent age increase with depth. The quartz separates gave D_e values between 0.6 ± 0.1 and 6.5 ± 0.2 Gy resulting in stratigraphically consistent OSL age estimates between 0.6 ± 0.1 and 7.1 ± 0.5 ka (Fig. 6).

At the Hon Gom 3 section, modern sand was sampled for testing the bleaching behaviour of the sediment. The D_e values yielded 5.9 ± 5.7 and 0.1 ± 0.1 Gy, as determined by MAAD and SAR protocol, respectively. The IRSL age estimates indicate a modern deposition of the sand, which is in agreement with the geological observation. The quartz separate gave a D_e value of 0.6 ± 0.1 Gy resulting in an OSL age estimate of 0.02 ± 0.01 ka.

Further south at the Suoi Tien section, similar dosimetric results were obtained for the sediments. The uranium, thorium, and potassium content ranging from 0.6 to 1.5 ppm, from 2.3 to 5.2 ppm, and from 0.05 to 0.9%. The dose rate is between 1.27 and 2.28 Gy/ka and between 0.49 and 1.35 Gy/ka for the feldspar and quartz separates, respectively. Due to intensive weathering and groundwater mobility, enrichment of radioisotopes in the lowermost layer, and thus radioactive disequilibrium in parts of the

Table 4 Equivalent dose and luminescence age results for the samples taken at Hon Gom and Suoi Tien sections

Sample	Palaeodose in Grey			Age in 1,000 years		
	Fsp-MAAD	Fsp-SAR	Qz-SAR	Fsp-MAAD	Fsp-SAR	Qz-SAR
HG1-1	7.7 ± 3.0	8.1 ± 0.2	7.4 ± 0.2	3.6 ± 1.4	3.8 ± 0.2	6.2 ± 0.3
HG1-2	7.0 ± 2.2	7.9 ± 0.1	6.1 ± 0.1	4.1 ± 1.4	4.7 ± 0.4	6.6 ± 0.3
			6.8 ± 0.2			7.3 ± 0.4
HG1-3	6.6 ± 2.4	7.9 ± 0.1	6.2 ± 0.1	4.0 ± 1.5	4.7 ± 0.3	6.5 ± 0.4
HG1-4	7.2 ± 1.7	7.9 ± 0.1	6.2 ± 0.1	4.0 ± 1.0	4.4 ± 0.3	6.5 ± 0.4
HG1-5	8.8 ± 1.7	9.8 ± 0.2	9.6 ± 0.3	4.5 ± 1.0	5.0 ± 0.5	8.3 ± 0.6
HG1-6	8.5 ± 2.5	9.1 ± 0.1	7.3 ± 0.1	4.3 ± 1.3	4.6 ± 0.4	6.2 ± 0.4
			7.9 ± 0.2			6.7 ± 0.5
HG2-1	7.3 ± 1.6	7.8 ± 0.1	6.5 ± 0.2	4.4 ± 1.0	4.7 ± 0.4	7.1 ± 0.5
HG2-2	2.3 ± 2.2/4.6 ± 0.7	3.9 ± 0.1	5.2 ± 0.2	0.8 ± 0.7	1.3 ± 0.1	2.6 ± 0.1
				1.5 ± 0.3		
HG2-3	1.4 ± 4.8	0.3 ± 0.1	0.6 ± 0.1	–	0.2 ± 0.1	0.6 ± 0.1
ST1	310.8 ± 3.4	290.6 ± 4.6	187.2 ± 10.0	136 ± 11	127 ± 10	139 ± 15
ST2	264.8 ± 4.9	224.5 ± 4.5	136.6 ± 6.9	208 ± 28	190 ± 27	276 ± 17
ST3	–	104.7 ± 2.1	75.3 ± 2.3	–	81.8 ± 9.5	122 ± 6
HG3-1	5.9 ± 5.7	0.1 ± 0.1	0.6 ± 0.1	1.5 ± 1.4	0.05 ± 0.05	0.02 ± 0.01

Fsp-MAAD feldspar separates measured by multiple aliquot additive dose protocol; *Fsp/Qz-SAR* feldspar/quartz separates, as measured by SAR protocol

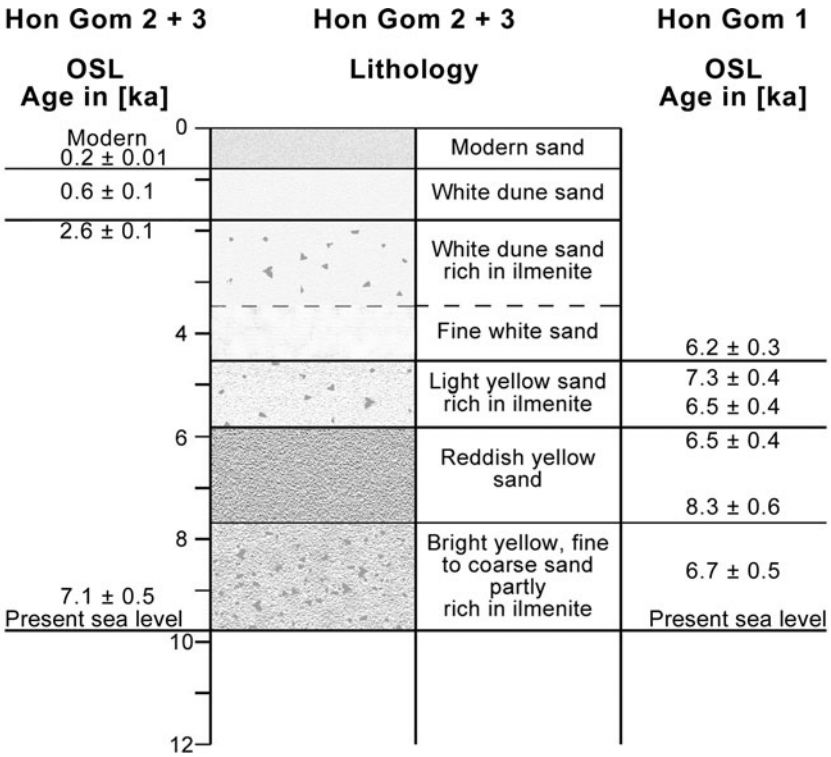

Fig. 6 OSL age estimates of the sand successions from Hon Gom sections 1–3

horizons, is likely. However, the measured isotopes do not indicate a radioactive disequilibrium for the sediments under study. The reddish yellow dune sand has a higher dose rate, most likely owing to the higher clay content. The dosimetric results of this study are in good agreement with those of Murray-Wallace et al. (2002) on sediments from the same section.

The feldspar separates yielded D_e values increasing with depth from 104.7 ± 2.1 to 290.6 ± 4.6 Gy and from 264.8 ± 4.9 to 310.8 ± 3.4 Gy, as determined by SAR and

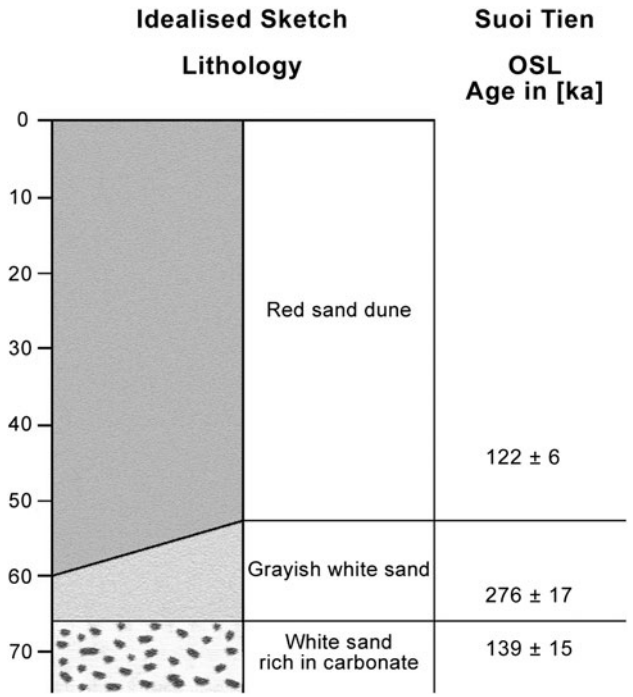

Fig. 7 OSL age estimates of the sand successions from Suoi Tien section

MAAD protocols, respectively (Fig. 7). The IRSL age estimates for the lower white sand rich in carbonate gave 127 ± 10 ka (SAR) and 136 ± 11 ka (MAAD). The upper greyish white sand yielded IRSL age estimates of 190 ± 27 ka (SAR) and 208 ± 28 ka (MAAD), whereas the red dune sand resulted in IRSL age estimate of 81.8 ± 9.5 ka (SAR). The quartz separates gave D_e values between 75.3 ± 2.3 and 187.2 ± 10.0 Gy resulting in OSL age estimates ranging from 122 ± 6 to 276 ± 17 ka. The OSL dates do not show an age increase with depth.

The age underestimation of feldspar separates compared to quartz separates ranges from 8.6 to 39.8%. The mean underestimation is about 30%, independently of the geological age of the studied material. This result could account for a fading rate of about 5% per decade.

Discussion

In central and SE Vietnam, the sand is attributed to long-term accumulation of fluvially derived sand transported to the continental shelf by rivers from the Truong Mountains during glacial and interglacial periods. This sand is subsequently reworked by wave activity and redeposited during interstadial and interglacial transgressions. The extensive reworking and re-deposition of aeolian sands implies intervals of reduced vegetation cover and landscape instability to permit sand remobilisation (e.g. Frechen et al. 2004; Porat et al. 2004). Schimanski and Stattegger (2005) calculated mass accumulation rates of 600–1,200 g/cm^3 per year in the shelf area for the time period of the early Holocene, which was caused by increased erosion in the Truong Son Mountains most likely due to intensified SW monsoon during the early Holocene. The outer barrier sands were deposited along the south-eastern coastline of Vietnam between about 8 and 6 ka, which is synchronous with the maximum sea-level high-stand after the postglacial marine transgression.

Tanabe et al. (2003) suggested that in the time period ranging from the LGM at about 20 ka to about 6 ka before present, the sea-level rapidly rose from approximately 120 m below the present sea-level to about 3 m above the present sea-level. Most of the dune sands exposed at the Hon Gom sections were deposited between 8.3 ± 0.3 and 6.2 ± 0.3 ka, as suggested by OSL dating results of this study (Fig. 8). Furthermore, Tanabe et al. (2003) suggested that sea-level was stable between 6 and 4 ka BP. Since 4 ka BP, the sea-level has dropped to the present level. Two younger periods of sand accumulation are recorded at 2.5 ± 0.1 and 0.2 ± 0.01 ka BP. Dune formation is still active in the study area.

At the Suoi Tien section, the white sand at the bottom of the sequence gave IRSL age estimates of 127 ± 10 and 190 ± 27 ka, OSL age estimates of 139 ± 15 and 276 ± 17 ka (Fig. 7), and a previously determined TL age estimate of >204 ka (Murray-Wallace et al. 2002). The upper greyish white sand yielded IRSL age estimates of 207 ± 34 and 244 ± 40 ka. Murray-Wallace et al. (2002) took one sample from this unit and gave a TL age estimate

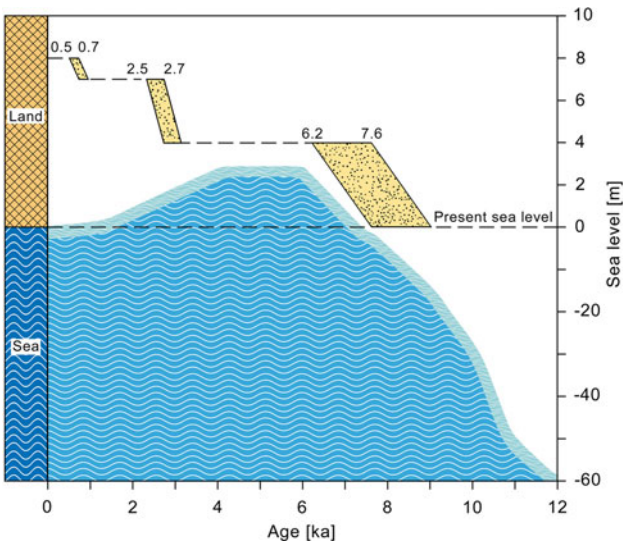

Fig. 8 Idealised sketch showing the correlation between sea-level change and sand accumulation, as determined by OSL dating. The sea-level curve is based on results of Schimanski and Stattegger (2005) and Tanabe et al. (2003)

of 48 ± 6 ka, which they excluded from age interpretation owing to the possibility of radioactive disequilibrium. Murray-Wallace et al. (2002) reported substantial problems concerning varying TL saturation levels between 204 and 48 ka due to the specific TL characteristics of quartz and partial bleaching of the TL signal of quartz. In this study, we have not observed a similar behaviour for IRSL and OSL. The potassium-rich feldspar, which was investigated in this study, does not seem to have the problem of varying saturation levels between 48 and 204 ka. The sediment was found to be in radioactive equilibrium by checking the isotopes listed in Table 3. However, difficulties following the tropical climate and subsequent weathering could result in the mobility of radioisotopes, and thus could result in radioactive disequilibrium at least in parts of the sequence, as described previously by Murray-Wallace et al. (2002).

The red dune sands yielded an IRSL age estimates of 101 ± 16 ka, which is in agreement with a TL age estimate of 85 ± 9 ka determined by Murray-Wallace et al. (2002). It is very likely that the yellowish red and red dune sand forming a coastal barrier succession was deposited during marine isotope substage (MIS) 5c or 5a, when sea-level was up to 20 m below the present level. At that time, the shore-line was 5–20 km off the recent coastline and large amount of sand (dunes) migrated considerable distances inland and accumulated along the southeast coast of Vietnam during periods of enhanced aeolian activity. At the Suoi Tien section, the deposition of the inner barrier sands correlate with an earlier sea-level high stand prior to the last glaciation. However, a simple correlation of these terrestrial sequences with sea-level fluctuations and the cold/warm cycles represented by the marine record is under discussion and most likely an oversimplification (cp Murray-Wallace 2002). The dunes are subsequently covered by multiphase renewed periods of sand accumulation, which cause a vertical growth and an elongated morphology of the dune system.

OSL dating of the aeolian deposits from the southeast and central coast of Vietnam provided a more reliable chronological frame for periods of increased aeolian sand mobility, which correlates with the onset of the maximum Holocene sea-level rise.

Conclusion

This study demonstrated the excellent suitability of dune sands and coastal sands from Vietnam for OSL dating and considerably contributed to the knowledge of the impact of sea-level change and climate change on the sedimentary environment along the coast. The depositional pattern and sedimentary facies are closely related to Holocene sea-level changes. In particular, the rising sea-level between 9 and 6 ka BP had a major impact on the evolution of coastal dynamics and periods of sand accumulation indicating a strong relation to climate change. Along the southeast coast of Vietnam, the deposition periods of inner barrier sands are correlated to an earlier sea-level high stand prior to the last interglacial maximum correlating to marine isotope substage 5e. The OSL dating study shows excellent agreement with geological estimates and data available from marine sediment cores from the shelf area off the coast in central and southeast Vietnam.

Acknowledgments D.Q.M. wishes to thank the technicians and staff from the Leibniz Institute for Applied Geosciences in Hannover. The study was in the frame of a PhD cooperation between JGEP (Joint Graduated Education Project), Hanoi University of Science, Vietnam, the Baltic Sea Research Institute, University of Greifswald and the Leibniz Institute for Applied Geosciences, Hannover. Funding was supported by Vietnam Ministry of Education and Training and Baltic Sea Research Institute.

References

Aitken MJ (1998) Introduction to optical dating. Academic Press, Oxford

Bøtter-Jensen L, McKeever SWS, Wintle AG (2003) Optically stimulated luminescence dosimetry. Elsevier, Amsterdam

Dao TM, Nguyen N (2001) Some features of geology and paleographic evolution of Hon-Gom peninsula. Vietnam J Geol 267 (in Vietnamese with English abstract)

Frechen M, Neber A, Tsatskin A, Boenigk W, Ronen A (2004) Chronology of Pleistocene sedimentary cycles in the Carmel Coastal Plain of Israel. Quat Int 121:41–52

Huntley DJ, Barril MR (1997) The K content of the K-feldspars being measured in optical dating or in thermoluminescence dating. Ancient TL 15:11–13

Jacobs Z (2008) Luminescence chronologies for coastal and marine sediments. Boreas 37:508–535

Kunz A, Frechen M, Ramachandran R, Urban B (2009) Chronological frame of coastal deposits from the South Andaman Islands, Bay of Bengal. Int J Earth Sci (this issue)

Lambeck K, Chappell J (2001) Sealevel change during the last glacial cycle. Science 292:679–686

Le-Duc T (2003) South China Sea. Hanoi (in Vietnamese)

Lian OB, Roberts RG (2006) Dating the quaternary: progress in luminescence dating of sediments. Quat Sci Rev 25:2449–2468

Madsen AT, Murray AS, Andersen TJ, Pejrup M, Breuning-Madsen H (2005) Optically stimulated luminescence dating of young estuarine sediments: a comparison with Pb-210 and Cs-137 dating. Mar Geol 214:251–268

Murray AS, Wintle AG (2000) Luminescence dating of quartz using an improved single-aliquot regenerative-dose protocol. Rad Meas 32:57–73

Murray-Wallace CV (2002) Pleistocene coastal stratigraphy, sealevel highstands and neotectonism of the southern Australian passive continental margin—a review. J Quat Sci 17:469–489

Murray-Wallace C, Jones BG, Nghi T, Price DM, Vu VV, Nguyen TT, Nanson GC (2002) Thermoluminescene ages for a reworked coastal barrier, southeastern Vietnam: a preliminary report. J Asian Earth Sci 20:535–548

Nghi T (1996) Evolution of Coastal sandy formations in Central Vietnam in relationship with oscillation of sea-level in Quaternary. Contributions Mar Geol and Geophy, vol II, Vietnam

Institute of Oceanography, Science and Technical Publishing house, Hanoi, pp 130–138 (in Vietnamese)
Nghi T (1998) Environment and forming mechanism of Phan Thiet Red sands. Vietnam Jour Geol 245(3–4):10–20 (in Vietnamese)
Nguyen DT (1998) Nha-Trang D-49-XXXII geological and mineral resources map of Vietnam on 1:200.000. Department of Geology and Minerals of Vietnam
Porat N, Avital A, Frechen M, Almogi-Labin A (2003) Chronology of upper quaternary offshore successions from the southeastern Mediterranean Sea, Israel. Quat Geochron 22:1191–1199
Porat N, Wintle AG, Ritte M (2004) Mode and timing of kurkar and hamra formation, central coastal plain, Israel. Israel J Earth Sci 53:13–25
Prescott JR, Hutton JT (1994) Cosmic ray contributions to dose rates for luminescence and ESR dating: large depths and long-term time variations. Rad Meas 23:497–500
Rabineau M, Berné S, Olivet JL, Aslanian D, Guillocheau F, Joseph P (2006) Palaeo sea levels reconsidered from direct observation of paleoshoreline position during glacial maxima (for the last 500,000 years). Earth Planet Sci Lett 253:119–137
Schimanski A, Stattegger K (2005) Deglacial and Holocene evolution of Vietnam shelf: stratigraphy, sediments and sea-level change. Mar Geol 214:365–387
Siddall M, Chappell J, Potter EK (2007) Eustatic sea level during past interglacials. Dev Quat Sci 7:75–92
Szczucinski W, Stattegger K (2001) Style and rate of shelf sedimentation offshore Nha-Trang, Vietnam, South China Sea. Meyniana 53:143–162
Tanabe S, Hori K, Saito Y, Haruyama S, Vu VP, Kitamura A (2003) Song Hong (Red River) Delta evolution related to millennium-scale Holocene sea-level changes. Quat Sci Rev 22:2345–2361
Tran T (1998) Tuy-Hoa D-49-XXVI geological and mineral resources map of Vietnam on 1:200.000, Department of Geology and Minerals of Vietnam
Vink A, Steffen H, Reinhardt L, Kaufmann G (2008) Holocene relative sea-level change, isostatic subsidence and the radial viscosity structure of the mantle of northwest Europe (Belgium, the Netherlands, Germany, southern North Sea). Quat Sci Rev 26:3249–3275
Waelbroeck C, Labeyrie L, Michel E, Duplessy JC, McManus JF, Lambeck K, Balbon E, Labracherie M (2002) Sealevel and deep water temperature changes derived from benthic foraminifera isotopic records. Quat Sci Rev 21:295–305
Wallinga J, Murray AS, Wintle AG (2000) The single-aliquot regenerative-dose (SAR) protocol applied to coarse-grain feldspar. Rad Meas 32:529–533
Wintle AG (1997) Luminescence dating: laboratory procedures and protocols. Rad Meas 27:769–817